Taylor Couette Instability in Sphere Suspensions

J. J. J. Gillissen and H. J. Wilson

Department of Mathematics, University College London,

Gower Street, London, WC1E 6BT.

E-mail: jurriaangillissen@gmail.com

(Dated: May 8, 2019)

Abstract

We employ a rheological theory to show that circular Taylor Couette flow of a suspension of non-Brownian spheres is less stable than that of a Newtonian fluid, at equal effective viscosity. The destabilisation is related to the preferred orientation of the separation vector of the closely interacting spheres, in the compressive direction of the base flow. The results agree qualitatively with experimental observations from the literature.

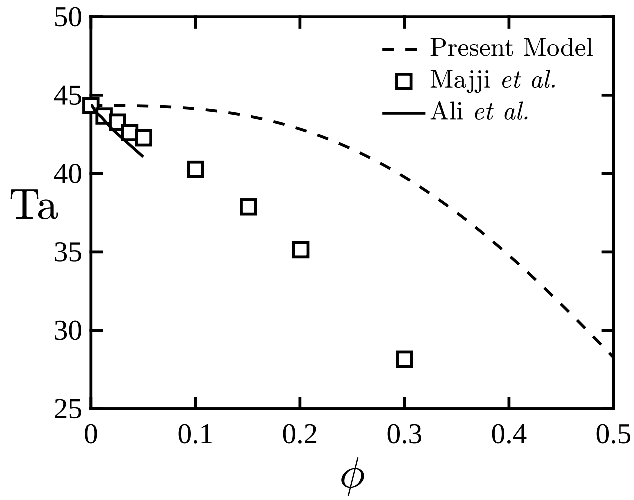

FIG. 1. The critical, effective Taylor number Ta [Eq. (1)] as a function of the sphere volume fraction ϕ, Comparison between the experimental data of Ref. [4] (markers), the two-fluid theory of Ref. [5] (solid line), and the present rheological theory (dashed line).

I. INTRODUCTION

Taylor Couette flow (TCF) is the flow between two concentric cylinders. When the outer cylinder is fixed, and when the rotation speed of the inner cylinder exceeds a critical value, the flow undergoes a centrifugal instability, and develops an array of axisymmetric vortices [1]. A further increase of the rotation speed induces bifurcations into more complicated (wavy, oscillatory, etc.) vortices, and eventually into a state of fully developed turbulence. Owing to the connection with turbulence, and owing to the tractability by linear stability analysis, TCF is the subject of a vast amount of literature [2]. There is particular interest in TCF instability for non-Newtonian fluids. For instance, predicting experimentally measured onset conditions for instability provides a stringent test in the development of constitutive equations for complex fluids; see e.g. Ref. [3].

In this work we study TCF of a suspension of non-Brownian spheres, which has experimentally been shown to be less stable than a Newtonian fluid, with equal effective viscosity [4]. These authors use a water-glycerol mixture, suspending density matched poly-methyl methacrylate spheres, with a radius of $a = 115$ μm, in the concentration rage $0 \leq \phi \leq 0.3$ and in a flow cell, with an inner radius of $R_1 = 100.3$ mm, and an outer radius of $R_2 = 114.3$ mm, i.e. a radius ratio of $R_2/R_1 = 1.14$. The sphere Reynolds number is $\dot{\gamma}a^2/\nu \sim 10^{-2}$, where ν is the suspending fluid kinematic viscosity, $\dot{\gamma} = U/\Delta R$ is the shear rate, $U = \Omega R_1$ is the velocity of the inner cylinder, and Ω is the rotation speed of the inner cylinder. The experimental results are plotted as a function of the sphere volume fraction ϕ in Fig. 1 with the markers, where the onset of instability is expressed by the effective, critical Taylor number:

$$\mathrm{Ta} = \frac{U \Delta R}{\nu_{\mathrm{eff}}} \sqrt{\frac{\Delta R}{R_1}}. \tag{1}$$

Here $\Delta R = R_2 - R_1$ is the gap width between the cylinders, and $\nu_{\mathrm{eff}}(\phi)$ is the concentration dependent and shear rate invariant, effective suspension viscosity, which was measured in Ref. [4], and was parameterised by:

$$\frac{\nu_{\mathrm{eff}}}{\nu} = \left(1 - \frac{\phi}{0.55}\right)^{-1.83}. \tag{2}$$

The reduction in the critical, effective Taylor number, observed in Fig. 1, indicates, that sphere suspensions are less stable than Newtonian liquids, with equivalent effective viscosities. At small sphere concentrations ϕ, this effect is believed to be related to the slip between the solid and the fluid phase, and the associated, inhomogeneous spatial sphere distribution [6].

At small ϕ, the destabilisation of TCF due to non-Brownian spheres has been captured by linear stability analysis of axisymmetric perturbations of the two fluid theory, using a radius ratio of $R_2/R_1 = 1.18$ [5]. Under the assumptions of $\phi \ll 1$, and a small sphere Reynolds number $\dot{\gamma} a^2/\nu \ll 1$, these authors adopt the following momentum equations for the liquid and solid phases:

$$\partial_t \boldsymbol{u} + \boldsymbol{u} \cdot \boldsymbol{\nabla} \boldsymbol{u} = -\boldsymbol{\nabla} p + \nu \nabla^2 \boldsymbol{u} + \phi \tau^{-1} (\boldsymbol{v} - \boldsymbol{u}), \tag{3a}$$

$$\partial_t \boldsymbol{v} + \boldsymbol{v} \cdot \boldsymbol{\nabla} \boldsymbol{v} = -\boldsymbol{\nabla} p + \tau^{-1} (\boldsymbol{u} - \boldsymbol{v}). \tag{3b}$$

Here $\boldsymbol{u}$ is the fluid velocity, $\boldsymbol{v}$ is the (locally averaged) sphere velocity, p is the fluid pressure, and $\tau = 2a^2/(9\nu)$ is the sphere relaxation time. In steady shear flow, the effective viscosity of the two fluid theory [Eq. (3)] equals $\nu_{\mathrm{eff}} = \nu$. Under time varying conditions, the magnitude of the interfacial drag force can be estimated, by ignoring the pressure term in Eq. (3b), and by assuming $\boldsymbol{u} = \hat{\boldsymbol{u}} \cos(\omega t)$, with $\hat{\boldsymbol{u}}$ and ω constants, such that the sphere velocity is governed by: $\dot{\boldsymbol{v}} = \tau^{-1} [\hat{\boldsymbol{u}} \cos(\omega t) - \boldsymbol{v}]$, which is solved by:

$$\phi \tau^{-1} (\boldsymbol{u} - \boldsymbol{v}) = -\phi \dot{\boldsymbol{u}}, \tag{4}$$

where it was furthermore used that $\omega\tau \ll 1$. Eq. (4) illustrates, that the interfacial drag force is independent of the sphere size, and ϕ is the only non-dimensional parameter that is introduced by the addition of the spheres.

The results of the linear stability analysis of Eq. (3) in TCF, are plotted in Fig. 1 by the solid line [5]. The data agree well with the experiments of Ref. [4] (markers). The theory [Eq. (3)] however is restricted to small ϕ and the computations of Ref. [5] were performed for $0 < \phi < 0.05$. For larger ϕ, sphere interactions play a role, and these effects are not captured by Eq. (3). These interactions give rise to extra stresses, which depend on the relative arrangement of the spheres, referred to as the microstructure; see e.g. Refs. [7, 8]. In this regard, it is known, that suspensions behave (generalised) Newtonian for $\phi \lesssim 0.2$, while for $\phi \gtrsim 0.2$, the anisotropic microstructure gives rise to deviations from Newtonian behaviour, with substantial normal stresses in shear flow. In these dense systems, the dominant effect of the spheres is expected to be an extra stress, while the interfacial drag force, described by Eq. (3), is expected to play an inferior role, as well as the associated inhomogeneity in the spatial sphere distribution. In this work we use our previously developed sphere stress theory, to investigate whether the above mentioned non-Newtonian stresses, that are important at large ϕ, either have a stabilising or a destabilising effect on the circular TCF.

II. HYDRODYNAMIC THEORY

The theory ignores all non-hydrodynamic forces, and expresses the extra stress, induced by the lubrication forces between the spheres [7]. This assumption is valid for a negligible sphere Reynolds number $\dot{\gamma}a^2/\nu \ll 1$, and for the intermediate volume fractions $0.2 < \phi < 0.4$, that are experimentally probed in Ref. [4], while at lower volume fractions the lubrication approximation fails, and at higher volume fractions direct contacts become important [8]. The purely hydrodynamic stress reads:

$$\boldsymbol{\sigma} = 2\nu\alpha\boldsymbol{s} : \langle\boldsymbol{nnnn}\rangle, \tag{5}$$

where $\boldsymbol{s} = \frac{1}{2}\left(\boldsymbol{\nabla u} + \boldsymbol{\nabla u}^T\right)$ is the rate of strain tensor, $\boldsymbol{\nabla u}$ is the velocity gradient tensor, $\boldsymbol{u}$ is the velocity vector, α is the stress parameter, which depends on ϕ, and is further specified in Eq. (11a), and $\langle\boldsymbol{nnnn}\rangle = \int \Psi(\boldsymbol{n})\boldsymbol{nnnn}d^2\boldsymbol{n}$, is the fourth order moment of the distribution Ψ of the sphere pair separation unit vector $\boldsymbol{n}$ (Fig. 2). In Eq. (5), there is no

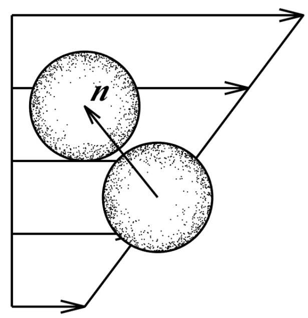

FIG. 2. The sphere pair separation unit vector $\boldsymbol{n}$.

explicit dependence of $\boldsymbol{\sigma}$ on the sphere radius a, since, in Stokesian systems, there are no variables to non-dimensionalise a with.

Under the assumption that Ψ is weakly anisotropic, $\langle \boldsymbol{nnnn} \rangle$ can be expressed as a linear function of the second order moment $\boldsymbol{a} = \langle \boldsymbol{nn} \rangle = \int \Psi(\boldsymbol{n}) \boldsymbol{nn} d^2\boldsymbol{n}$ as follows [9]:

$$
\begin{aligned}
\langle n_i n_j n_k n_l \rangle = & -\tfrac{1}{35} \langle n_m n_m \rangle \left(\delta_{ij}\delta_{kl} + \delta_{ik}\delta_{jl} + \delta_{il}\delta_{jk} \right) \\
& + \tfrac{1}{7} \Big(\delta_{ij} \langle n_k n_l \rangle + \delta_{ik} \langle n_j n_l \rangle + \delta_{il} \langle n_j n_k \rangle + \langle n_i n_j \rangle \delta_{kl} + \langle n_i n_k \rangle \delta_{jl} + \langle n_i n_l \rangle \delta_{jk} \Big),
\end{aligned}
$$

such that the non-isotropic part of the sphere stress [Eq. (5)] reads:

$$
\frac{\boldsymbol{\sigma}}{2\nu\alpha} = -\tfrac{2}{35} \boldsymbol{s} + \tfrac{2}{7} \left(\boldsymbol{s} \cdot \boldsymbol{a} + \boldsymbol{a} \cdot \boldsymbol{s} \right). \tag{6}
$$

In xy-shear flow with shear rate $\dot{\gamma}$:

$$
\boldsymbol{s} = \frac{\dot{\gamma}}{2} \begin{pmatrix} 0 & 1 & 0 \\ 1 & 0 & 0 \\ 0 & 0 & 0 \end{pmatrix}, \tag{7}
$$

the distribution Ψ is assumed a superposition of isotropic and preferred alignment with the compressive axis $\boldsymbol{n}^c = (-1, 1, 0)/\sqrt{2}$ [10]:

$$
\boldsymbol{a} = \frac{1-\beta}{3} \boldsymbol{\delta} + \beta \boldsymbol{n}^c \boldsymbol{n}^c = \begin{pmatrix} \frac{1}{3} + \frac{\beta}{6} & -\frac{\beta}{2} & 0 \\ -\frac{\beta}{2} & \frac{1}{3} + \frac{\beta}{6} & 0 \\ 0 & 0 & \frac{1}{3} - \frac{\beta}{3} \end{pmatrix}, \tag{8}
$$

where β is the anisotropy parameter. Combining Eqs. (6, 8), gives the following stress in shear flow:

$$\frac{\boldsymbol{\sigma}}{2\nu\dot{\gamma}\alpha} = \begin{pmatrix} -\frac{\beta}{7} & \frac{(5\beta+7)}{105} & 0 \\ \frac{(5\beta+7)}{105} & -\frac{\beta}{7} & 0 \\ 0 & 0 & 0 \end{pmatrix}, \tag{9}$$

which reduces to a Newtonian stress for $\beta = 0$, and which corresponds to the following effective viscosity:

$$\frac{\nu_{\text{eff}}}{\nu} - 1 = \frac{\sigma_{12}}{\nu\dot{\gamma}} = \alpha\frac{2(5\beta+7)}{105}, \tag{10a}$$

and the following, relative, second normal stress difference:

$$\zeta_2 = \frac{\sigma_{22} - \sigma_{33}}{\sigma_{12}} = -\frac{15\beta}{5\beta+7}, \tag{10b}$$

and the first normal stress difference is zero by construction $\zeta_1 = (\sigma_{11} - \sigma_{22})/\sigma_{12} = 0$, in qualitative agreement with the experimental literature. In this work we tune α and β as:

$$\alpha = \frac{5\left(3 - 2\phi^2\right)}{2}\left[\left(1 - \frac{\phi}{0.55}\right)^{-1.83} - 1\right], \tag{11a}$$

and:

$$\beta = \frac{14\phi^2}{5\left(3 - 2\phi^2\right)}, \tag{11b}$$

such that Eq. (10) corresponds to the empirical effective suspension viscosity ν_{eff}/ν [Eq. (2)], and relative, second normal stress difference:

$$\zeta_2 = -2\phi^2. \tag{12}$$

It is emphasised that with Eq. (11), the theory [Eqs. (6, 8)] exactly reproduces experimentally measured shear stress and second normal stress difference. It is noted, that contact forces may result in a positive first normal stress difference [8]. Here we ignore these effects, and restrict our focus to purely hydrodynamic systems, for which the non-Newtonian rheology is dominated by the second normal stress difference, i.e. $|\zeta_2| \gg |\zeta_1|$, as is usually observed in shear rate invariant sphere suspensions [11–14].

III. STABILITY ANALYSIS

TCF is described in cylindrical coordinates: $r, \theta, z = 1, 2, 3$, and is governed by the continuity equation:

$$\boldsymbol{\nabla} \cdot \boldsymbol{u} = 0, \tag{13}$$

and the momentum equation:

$$\partial_t \boldsymbol{u} = \boldsymbol{\nabla} \cdot \left[-\boldsymbol{u}\boldsymbol{u} - p\boldsymbol{\delta} + \nu \left(\boldsymbol{\nabla}\boldsymbol{u} + \boldsymbol{\nabla}\boldsymbol{u}^T \right) + \boldsymbol{\sigma} \right]. \tag{14}$$

The velocity gradient tensor in cylindrical coordinates reads:

$$\nabla_i u_j = \begin{pmatrix} \partial_r u_r & \partial_r u_\theta & \partial_r u_z \\ -r^{-1} u_\theta & r^{-1} u_r & 0 \\ \partial_z u_r & \partial_z u_\theta & \partial_z u_z \end{pmatrix}. \tag{15}$$

We compute the linear stability of the laminar solution to Eqs. (6, 8, 13, 14), w.r.t. axisymmetric perturbations, that are harmonic functions of z, with a wavenumber k. Although non-axisymmetric modes are observed in the experiments of Ref. [4], axisymmetric modes serve the purpose of the present work, of elucidating the basic destabilising mechanism of the particle stress, due to the anisotropic microstructure. We decompose the fluid velocity: $\boldsymbol{u} = \boldsymbol{U}(r) + \boldsymbol{u'}(r,t)\exp(ikz)$, into a base state, denoted by a capital letter: $\boldsymbol{U}$, and a perturbation, denoted by a prime: $\boldsymbol{u'}\exp(ikz)$.

The base state has a Newtonian character, which corresponds to a shear rate invariant and position invariant effective viscosity ν_{eff}, which is given by Eq. (2). The corresponding velocity field: $\boldsymbol{U} = U_\theta \boldsymbol{e}_\theta$, is governed by the azimuthal component of the momentum equation [Eq. (14)]: $\left(\partial_r + 2r^{-1}\right)\left(\partial_r - 2r^{-1}\right) U_\theta = 0$, which gives:

$$U_\theta = \frac{\Omega r}{1 - R_2^2/R_1^2} + \frac{R_1^2 \Omega / r}{1 - R_1^2/R_2^2}. \tag{16}$$

The perturbations are governed by the continuity equation [Eq. (13)]:

$$\left(\partial_r + r^{-1}\right) u'_r + ik u'_z = 0, \tag{17}$$

and by the linearised momentum equations [Eq. (14)]:

$$\partial_t u'_r = -\partial_r p' + \nu \left(\partial_r^2 + r^{-1}\partial_r - r^{-2} - k^2\right) u'_r + 2r^{-1} U_\theta u'_\theta + \left(\partial_r + r^{-1}\right)\sigma'_{rr} + ik\sigma'_{zr} - r^{-1}\sigma'_{\theta\theta}, \tag{18}$$

$$\partial_t u'_\theta = \nu \left(\partial_r^2 + r^{-1}\partial_r - r^{-2} - k^2\right) u'_\theta - \left[\left(\partial_r + r^{-1}\right) U_\theta\right] u'_r + \left(\partial_r + 2r^{-1}\right)\sigma'_{r\theta} + ik\sigma'_{z\theta}, \tag{19}$$

and:

$$\partial_t u'_z = -ikp' + \nu \left(\partial_r^2 + r^{-1}\partial_r - k^2\right) u'_z + \left(\partial_r + r^{-1}\right)\sigma'_{rz} + ik\sigma'_{zz}, \tag{20}$$

and the perturbed stress [Eq. (6)] reads:

$$\frac{\boldsymbol{\sigma}'}{2\nu\alpha} = -\tfrac{2}{35}\boldsymbol{s}' + \tfrac{2}{7}\left(\boldsymbol{s}'\cdot\boldsymbol{a} + \boldsymbol{a}\cdot\boldsymbol{s}'\right), \tag{21}$$

where $\boldsymbol{s} = \frac{1}{2}\left(\boldsymbol{\nabla u} + \boldsymbol{\nabla u}^T\right)$, and the cylindrical components of the velocity gradient $\boldsymbol{\nabla u}$ are given in Eq. (15), and the cylindrical components of the conformation tensor $\boldsymbol{a}$ are identical to the Cartesian components, which are given in Eq. (8). We numerically solve the r-dependent velocity perturbations $\boldsymbol{u}'$ using Chebyshev discretisation on 30 collocation points [15]. We fix the Couette cell radius ratio to: $R_2/R_1 = 1.14$, similar as in the experimental study of Ref. [4].

The velocity perturbation evolution equations [Eqs. (16 - 21)] including the boundary conditions ($\boldsymbol{u}' = \boldsymbol{0}$ on the walls) are written in matrix form:

$$\boldsymbol{M}_1 \cdot \partial_t \boldsymbol{q}' = \boldsymbol{M}_2 \cdot \boldsymbol{q}', \tag{22}$$

and the growth rates are found by solving the corresponding generalised eigenvalue problem in FORTRAN using the ZGGEV routine from the LAPACK library. For all cases discussed below, the eigenvalue of the most unstable axisymmetric mode is real-valued, i.e. non-oscillatory.

The rotation rate Ω is varied to find the onset of instability, which correspond to a sign change of the largest eigenvalue. The onset point is expressed by the effective, critical Taylor number Ta [Eq. (1)].

IV. RESULTS

Fig. 3 shows the computed Ta as a function of the spanwise wavenumber $k\Delta R/\pi$ for Newtonian flow (sphere volume fraction $\phi = 0$) and for a suspension with $\phi = 0.5$. It is seen, that for both cases, the minimum, critical, effective Taylor number occurs at $k\Delta R/\pi \approx 1$. It is furthermore seen, that the spheres are destabilising, i.e. for $\phi = 0.5$, the predicted, critical, effective Taylor number is reduced by roughly 40%.

Fig. 4 shows the velocity components of the most unstable mode, in Newtonian flow ($\phi = 0$) at the critical Taylor number of Ta ≈ 44, and in a suspension with $\phi = 0.5$, at the critical, effective Taylor number of Ta ≈ 28. Note that these modes are normalised, and their magnitude has no physical significance. In both cases, the modes are similar, and are

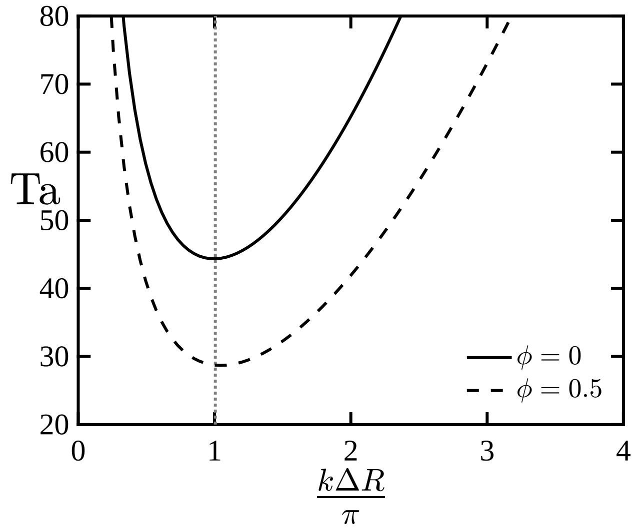

FIG. 3. The computed, critical, effective Taylor number Ta [Eq. (1)] as a function of the spanwise wavenumber $k\Delta R/\pi$, for Newtonian flow (sphere volume fraction $\phi = 0$; solid line) and for a suspension with $\phi = 0.5$ (dashed line). The vertical line indicates the minima of the curves.

dominated by the azimuthal velocity component. The the ratio of the cross-stream velocity fluctuations to the azimuthal velocity fluctuations is slightly larger in the suspension than in the Newtonian flow.

Fig. 1 shows the computed, critical, effective Taylor number for the suspension (dashed line) as a function of the sphere volume fraction ϕ. The figure shows, that, when compared at equal ν_{eff}/ν, the spheres have a destabilising effect for $\phi \gtrsim 0.2$, and a negligible effect for $\phi \lesssim 0.2$. This concentration dependence correlates with the non-Newtonian nature of the suspension, which is characterised by the second normal stress difference ζ_2 [Eq. (12)], which is non-negligible, only for $\phi \gtrsim 0.2$.

The destabilisation can be understood by the alignment of the microstructure with the base deformation [Eq. (8)]. To this end, we introduce an alternative definition for the effective "base flow viscosity" ν_{eff}, as the ratio of the dissipation of the base kinetic energy, due to the total (sphere plus solvent) stress and due to the solvent stress:

$$\nu_{\text{eff}} - 1 = \frac{\boldsymbol{S} : \boldsymbol{\Sigma}}{2\nu \boldsymbol{S} : \boldsymbol{S}}. \tag{23}$$

By inserting for $\boldsymbol{S}$ the expression for the base deformation rate [Eq. (7)] and for $\boldsymbol{\Sigma}$ the expression for the base particle stress [Eq. (9)], Eq. (23) reduces to Eq. (10a). Similarly, we introduce the effective "vortex viscosity" ν', which is based on the dissipation of the

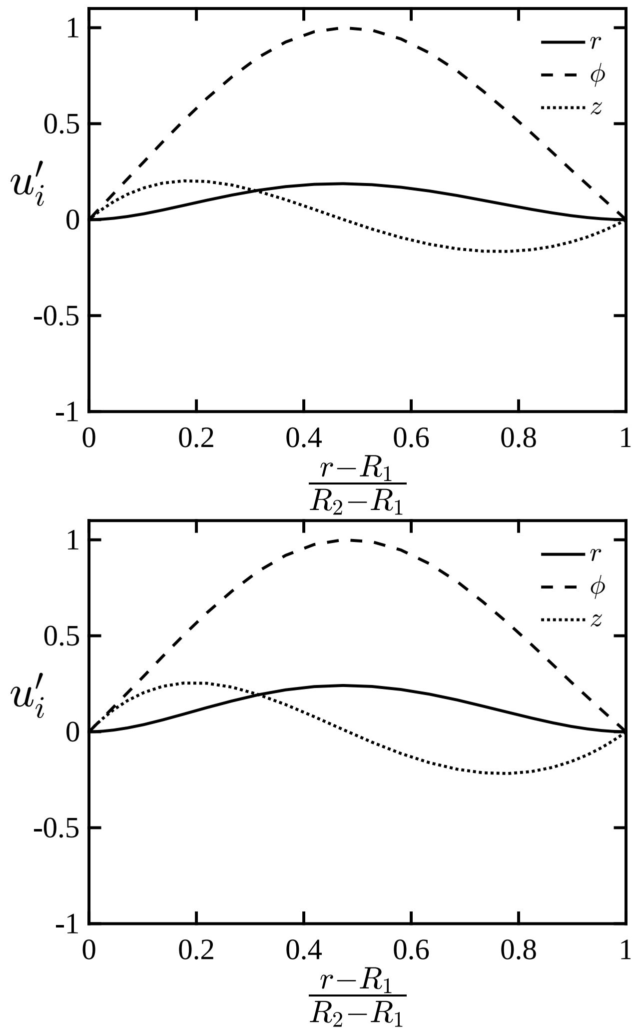

FIG. 4. (top) Most unstable eigenmode in Newtonian flow, i.e. using a sphere volume fraction of $\phi = 0$, and a Taylor number [Eq. (1)] at the critical value of Ta ≈ 44. (bottom) Most unstable axisymmetric eigenmode in a sphere suspension, using a sphere volume fraction of $\phi = 0.5$, and an effective Taylor number [Eq. (1)] at the critical value of Ta ≈ 28.

perturbed kinetic energy:

$$\nu' - 1 = \frac{\boldsymbol{s}' : \boldsymbol{\sigma}'}{2\nu \boldsymbol{s}' : \boldsymbol{s}'}. \tag{24}$$

Inserting the expressions for the perturbed stress $\boldsymbol{\sigma}'$ [Eqs. (8, 21)] into Eq. (24) gives:

$$\nu' - 1 = \alpha \left[\frac{2}{15} + \frac{4\beta}{7} \left(-\frac{1}{3} + \xi \right) \right],$$

where the alignment factor:

$$\xi = \frac{\boldsymbol{s}' : (\boldsymbol{s}' \cdot \boldsymbol{n}^c \boldsymbol{n}^c)}{\boldsymbol{s}' : \boldsymbol{s}'},$$

measures the deformation of the secondary flow in the compressive direction of the base flow. For perfectly aligned biaxial deformation, we see that $\xi = \frac{1}{2}$ and $\nu' = \nu_{eff}$. Since the secondary flow deformation is not perfectly aligned with the base flow deformation, we see that $\xi < \frac{1}{2}$. This means, that $\nu_{\text{eff}} > \nu'$, i.e. the spheres impose more friction to the base flow than to the secondary vortices. Since the instability involves the dynamics of the vortices, we may model the onset by $\text{Ta}' \approx 44$, where Ta' is the critical Taylor number, that is based on ν', i.e. $\text{Ta}' = (U\Delta R/\nu')\sqrt{\Delta R/R_1}$. Since $\nu_{\text{eff}} > \nu'$, this corresponds to a critical Taylor number based on ν_{eff}, that is smaller than the Newtonian value, i.e. $\text{Ta} = (U\Delta R/\nu_{\text{eff}})\sqrt{\Delta R/R_1} < 44$, which explains the destabilising effect.

The theoretical results in Fig. 1 (dashed line) show less destabilisation, as compared to the experiments in Ref. [4] (markers). As discussed above, part of the discrepancy may be explained by sphere inertia. Another possible cause for the discrepancy is the assumption of axisymmetry of the instability modes. For small volume fractions $\phi < 0.05$, this assumption agrees with the experiments of Ref. [4], and in this regime the discrepancy is therefore most likely due to neglecting inertia. This is confirmed by the agreement between the axisymmetric two-fluid theory [5], and the experimental data for $\phi < 0.05$ (see Fig. 1. At larger ϕ, the two-fluid theory does not hold, and to better capture this regime, we propose for future work, a non-axisymmetric stability analysis, that includes both particle inertia and particle stress, by combining the two fluid theory [Eq. (3)], with our particle stress theory [Eqs. (6, 8)].

V. CONCLUSIONS

In conclusion, we have theoretically predicted a destabilisation of the circular Taylor Couette flow w.r.t. axisymmetric perturbations, due to the presence of non-Brownian spheres. The non-Newtonian character of the suspension base flow, is characterised by the second normal stress difference, while the first normal stress difference is assumed zero. The destabilisation can be understood by the alignment between the microstructure and the base deformation.

ACKNOWLEDGMENTS

We would like to acknowledge financial support from the Engineering and Physical Sciences Research Council of the United Kingdom Grant No. EP/N024915/1.

---

[1] G I Taylor, "Stability of a viscous liquid contained between two rotating cylinders," Phil. Trans. R. Soc. Lond. Ser. A **223**, 289–343 (1923).

[2] MA Fardin, C Perge, and N Taberlet, "The hydrogen atom of fluid dynamics–Introduction to the Taylor–Couette flow for soft matter scientists," Soft Matter **10**, 3523–3535 (2014).

[3] JJJ Gillissen and HJ Wilson, "Taylor Couette instability in disk suspensions," Phys. Rev. Fluids **3**, 113903 (2018).

[4] Madhu V Majji, Sanjoy Banerjee, and Jeffrey F Morris, "Inertial flow transitions of a suspension in Taylor–Couette geometry," J. Fluid Mech. **835**, 936–969 (2018).

[5] Mohamed E Ali, Deepanjan Mitra, John A Schwille, and Richard M Lueptow, "Hydrodynamic stability of a suspension in cylindrical Couette flow," Phys.Fluids **14**, 1236–1243 (2002).

[6] Madhu V Majji and Jeffrey F Morris, "Inertial migration of particles in Taylor-Couette flows," Phys. Fluids **30**, 033303 (2018).

[7] JJJ Gillissen and HJ Wilson, "Modeling sphere suspension microstructure and stress," Phys. Rev, E **98**, 033119 (2018).

[8] JJJ Gillissen and HJ Wilson, "The effect of normal contact forces on the stress in shear rate invariant particle suspensions," Phys. Rev. Fluids **4**, 013301 (2019).

[9] E J Hinch and L G Leal, "Constitutive equations in suspension mechanics. Part 2. Approximate forms for a suspension of rigid particles affected by Brownian rotations," J. Fluid Mech. **76**, 187–208 (1976).

[10] Frédéric Blanc, Elisabeth Lemaire, Alain Meunier, and François Peters, "Microstructure in sheared non-Brownian concentrated suspensions," J. Rheol. **57**, 273–292 (2013).

[11] Anugrah Singh and Prabhu R Nott, "Experimental measurements of the normal stresses in sheared Stokesian suspensions," J. Fluid Mech. **490**, 293–320 (2003).

[12] Isidro E Zarraga, Davide A Hill, and David T Leighton Jr, "The characterization of the total stress of concentrated suspensions of noncolloidal spheres in Newtonian fluids," J. Rheol. **44**,

185–220 (2000).

[13] Étienne Couturier, François Boyer, Olivier Pouliquen, and Élisabeth Guazzelli, "Suspensions in a tilted trough: second normal stress difference," J. Fluid Mech. **686**, 26–39 (2011).

[14] Shao-Cong Dai, Erwan Bertevas, Fuzhong Qi, and Roger I Tanner, "Viscometric functions for noncolloidal sphere suspensions with newtonian matrices," J. Rheol. **57**, 493–510 (2013).

[15] C Canuto, M Y Hussaini, A Quarteroni, and A Thomas Jr, *Spectral Methods in Fluid Dynamics* (Springer Science & Business Media, 2012).